TRENDS IN SCIENCES 2025; 22(6): 9769 RESEARCH ARTICLE
https://doi.org/10.48048/tis.2025.9769

Droplet Combustion Behavior of Vegetable Oil Surrogate Fuel Enhanced with Alcohols

Lilis Yuliati[1,*], Ibrahim Ahmad Ibadurrohman[2], Nurkholis Hamidi[1], Mega Nur Sasongko[1], Widya Wijayanti[1] and Winarto[1]

[1]Department of Mechanical Engineering, Brawijaya University, East Java 65145, Indonesia
[2]Research Center for Energy Conversion and Conservation, National Research and Innovation Agency, South Tangerang 15314, Indonesia

([*]Corresponding author's e-mail: lilis_y@ub.ac.id)

Received: 13 January 2025, Revised: 25 February 2025, Accepted: 4 March 2025, Published: 5 May 2025

Abstract

Internal combustion engines play an essential role in industry and transportation due to their reliability, efficiency, and cost-effectiveness. However, emissions produced from fossil fuels impact environmental degradation, so alternative fuels are needed to increase combustion efficiency and reduce emissions. Vegetable oil is introduced as a renewable energy source, which is potentially used as a substitute for diesel fuel. However, vegetable oils are not fully compatible with diesel fuels, although they have some advantages regarding their properties. Therefore, this work aims to study the mechanism and enhancement of the single isolated droplet combustion behavior of oleic acid as the vegetable oil surrogate compound by adding 20 vol% of alcohol with different molecular structures. The droplet was suspended on the fiber to observe the combustion behavior under static conditions. The droplet dynamics and microexplosive behavior are investigated using spatial and temporal tracking under atmospheric pressure and normal gravity conditions. The post-processing procedure was used to observe the evolution of flame and droplet diameter. The fuel blends exhibit severe volumetric expansion followed by child droplet ejection with various droplet breakup structures due to different nucleation modes. This mechanism is essential to enlarge the fuel reaction zone with ambient air, which shortens the droplet lifetime with a lower ignition point. Methanol significantly reduces the droplet lifetime, while only 2-propanol reduces the ignition delay and burning lifetime among alcohol additives. Methanol addition generates the highest droplet peak temperature due to the faster burning rate, even though it has a lower energy density. Alcohol increases the flame standoff ratio due to the microexplosive behavior. During the unsteady and quasi-steady combustion phases, an elongated flame structure is formed due to natural convection, which is also related to soot formation. Alcohol diminishes the sooting propensity of oleic acid combustion with lower flame luminosity.

Keywords: Renewable energy, Droplet combustion, Oleic acid, Alcohol, Microexplosive behavior, Volumetric expansion, Nucleation modes, Soot formation, Flame standoff ratio, Flame luminosity

Introduction

Internal combustion engines will continue to play a vital role in powering industry and transportation in the future due to their great reliability and efficiency, high-power output, and lower operation cost [1]. Compression ignition (CI) engines commonly utilize liquid fuels due to their benefits, including their easy handling and storage, high energy content, and easily regulated combustion. Nevertheless, liquid fuel combustion, such as diesel fuel, tends to generate soot aggregate during combustion, significantly contributing to environmental degradation and climate change. Finding alternative fuels that can either substitute or augment conventional hydrocarbon-based fuels to minimize emissions and generate more ecologically

sustainable combustion [2-4]. The purpose of exploring renewable fuel sources has 2 major focuses, consisting of greenhouse emission reduction and providing an alternative to fossil fuels [5].

Bio-alcohols can be added to diesel fuels to introduce renewable fractions and to increase oxygen content to a certain level. Increasing oxygen concentration within the fuel blend improves combustion performance and reduces emission levels. Another option is to utilize vegetable oil directly used in internal combustion engines or transform it into biodiesel or hydrotreated vegetable oil as a potential substitute for diesel fuel [6-8]. Vegetable oils are advantageous for use as diesel fuel because of their renewable nature, contain less sulfur and aromatic, have a higher flash point for safer storage, have greater lubricity for better fuel pump performance, and have higher biodegradability and non-toxicity. However, vegetable oils are not fully compatible with automotive diesel fuel due to some drawbacks related to certain properties. Vegetable oil with a higher density and kinematic viscosity than diesel fuel will prohibit fuel atomization and produce large droplet sizes, which will cause a slower fuel evaporation rate and incomplete combustion [9,10]. Several methods have been utilized to reduce the viscosity of vegetable oil, such as preheating, conversion into biodiesel through transesterification, and blending with low-viscosity fuels [11]. The fuel additive is one of the most extensively used and promising strategies for modifying fuel properties to enhance engine performance without requiring engine modification [4]. High-volatility and low-volatility constituents as droplet fuel mixtures potentially promote secondary atomization that encourages a faster burning rate due to explosive boiling within the superheated liquid [12]. Many empirical and theoretical investigations have been carried out employing the isolated droplet combustion method to gain new insight into the physical and chemical mechanism of burning multi-component fuels [13].

After being injected into the combustion chamber of a diesel engine, the fuel breaks up and disperses into a large population of small droplets. Spray combustion involves intricate multi-dimensional aerodynamic phenomena encompassing 2-phase flow of multicomponent, heat and mass transport, chemical reactions, and phase change. Studying spray combustion in engines is very complicated because fuel droplets of different sizes are dispersed randomly, and many processes occur simultaneously. Therefore, the isolated droplet technique is proposed as the most straightforward approach to comprehending the spray behavior involving multiple and complex processes, treating spray as an aggregation of a large droplet population. [14-16]. A significant gap still exists between spray and droplet combustion. Despite extensive research on droplet combustion, many findings have not been effectively utilized to clarify the spray combustion mechanism [17]. Understanding the dynamic behavior of a single droplet is critical for converting fundamental discoveries of the ignition and combustion of liquid fuels into practice areas. Although a single droplet case seems idealized, this assumption is appropriate for most combustion devices when the spray may be regarded as diluted. This method contributes to a better understanding of the more complicated spray combustion processes encountered in many combustion devices [18-21].

A previous study investigated the combustion of biodiesel-butanol droplets, revealing that microexplosions occurred in 2 distinct modes. The first, referred to as the core mode, involved a periodic bubble nucleation, expansion, and rupture within the droplet. The second, called the surface mode, was characterized by the formation of numerous micron-sized child droplets [22]. Another study was conducted on a biodiesel and diesel-based fuel blended with 3 different alcohols to investigate the binary and multiple fuel components. The average burning rates for binary components increased due to microexplosion, and biodiesel-methanol fuel blends yield a higher microexplosion possibility [23]. The previous study discovered that at a 50 vol% ethanol content, the droplet combustion of the biodiesel-ethanol fuel blend has the highest microexplosion strength with the lowest microexplosion delay time [24]. The effectiveness of microexplosion in improving fuel atomization may be assessed by the measurement of microexplosion delay time [25]. The previous investigation found that a 30 % ethanol addition to palm oil enhanced the burning rate constant by up to 23.2 % [26].

Most of the previous studies used biodiesel and vegetable oil as the base fuels to determine the role of alcohol in the combustion mechanism and the droplet

combustion behavior enhancement. These fuels are multi-component compounds with different boiling points. Hence, microexplosion still occurs even in the absence of alcohol additives [15,27,28]. It resulted in a complicated analysis to define whether the microexplosion occurred only due to the alcohol additives or the interaction between the base fuel constituents. On the other hand, 1 type of vegetable oil could have different concentrations of fatty acid composition, which are influenced by climatic conditions, growing seasons, and plant age [29]. The particular content of the fatty acids could have an opposite effect on fuel properties [30], resulting in favorable properties while having undesirable effects on other properties [31]. In some cases, minor fatty acid constituents exert a much stronger effect on fuel properties than indicated by the relative concentrations [32]. Therefore, Meiri *et al.* [33] propose using a single constituent to characterize biodiesel fuels or vegetable oils.

The number of carbon chains and C=C double bonds determined the distinctive properties of vegetable oils from different raw materials. Almost all fatty acid structures derived from plant and animal-based oils have 18 carbon chain lengths with double bonds between 0 and 3 [34]. As a multi-component fuel, vegetable oil has exclusive physicochemical characteristics determined by fatty acid properties as constituents. Viscosity and density are 2 essential properties to be considered in combustion, which relate to the spray quality and energy content of the fuel. Low density and viscosity result in reduced engine power output. However, excessively high viscosity has a negative impact on the effectiveness of fuel atomization [35-37]. The evaporation of multi-component fuel droplets involves more intricate heat and mass transport processes than single-component fuel. A single constituent of FA was chosen as a vegetable oil surrogate to simplify the study of vegetable oils and their combustion behavior. In previous studies, oleic acid (OA) was chosen because it is sustainable and made from non-edible sources, agricultural by-products, and waste feedstocks [15,38]. Oleate is an unsaturated species with 18 carbon chains and 1 C=C double bond between carbon atom numbers 8 and 9 [39]. Oleic acid, as a mono-unsaturated FA, has better oxidative stability than polyunsaturated FAs, such as linoleic and linolenic acid [30]. Oleic acid is abundant in many vegetable oils, such as olive oil (74.52 wt%), rapeseed oil (62.24 wt%), canola oil (60.33 wt%), jatropha oil (42.81 wt%), and palm oil (40.91 wt%) [31].

Vegetable oil as an alternative to diesel fuel has drawbacks that will deteriorate the engine performance. Consequently, the fuel blend is the most straightforward method to enhance the fuel properties suitable for the engine requirements. In this study, we employ oleic acid as the surrogate compound of vegetable oils, blending it with 4 types of alcohols with different carbon chain lengths, consisting of methanol, ethanol, 2-propanol, and n-butanol. Referring to a previous study, Pan and Chiu [23] pointed out in their experimental findings that higher volatility of short-chain alcohol leads to more severe microexplosion and higher burning rates. On the other hand, a comprehensive review by Lee *et al.* [40] reported that short-chain alcohol reduces the overall energy content of the fuel blend due to the abundant oxygenated compound. Therefore, this study investigates the effects of alcohol with different carbon chain lengths to determine the most efficient fuel blend with a significant enhancement in combustion behavior. This study uses the isolated droplet combustion method to simplify complex spray combustion and gain an understanding of the fuel droplet combustion behavior. The quantitative analysis is studied, and some phenomena between oleic acid and alcohol are discussed to introduce the mechanism and interaction of the fuel blend combustion.

Materials and methods

Materials and fuel preparation

Oleic acid (OA, 96 % purity) as the base fuel and surrogate compound was used to represent the dominant constituents of vegetable oil. OA is then mixed with 4 types of alcohol consisting of methanol (M, 99.99 % purity), ethanol (E, 99.8 % purity), 2-propanol (P, 99.98 % purity), and n-butanol (B, 99.95 % purity). The alcohol concentration is 20 vol% of the total mixture. A magnetic stirrer was used to produce homogeneous fuel blends between OA and alcohol. This process is done for 15 min at ambient temperature with a medium agitation rate. The fuel blends were kept in an enclosed container for 2 weeks to ensure the homogeneity of fuel blends without phase separation. The physical and chemical properties of the investigated material for the droplet combustion test are shown in **Table 1**.

Table 1 The physical and chemical properties of the analyzed fuel [6,23,38,41,42].

Properties	Oleic acid	Methanol	Ethanol	2-propanol	N-butanol
Molecular formula	$C_{18}H_{34}O_2$	CH_4O	C_2H_6O	C_3H_8O	$C_4H_{10}O$
C:H:O (wt%)	76.6:12.1:11.3	37.49:12.58:49.93	52.14:13.13:34.73	59.96:13.42:26.62	64.82:13.60:21.58
Molecular weight (g/mol)	282.46	32.04	46.07	60.1	74.12
Higher heating value (MJ/kg)	39.62	22.88	29.67	33.6	36.11
Boiling point (℃)	360	65	78.3	82.5	117.5
Melting point (℃)	16	−97.6	−114	−89	−90
Flash Point (℃)	189	12	8	11.7	35
Density (g/cm^3)	0.890	0.796	0.789	0.803	0.808
Kinematic viscosity (mm^2/s)	16.89	0.59	1.08	1.76	2.63

Experimental setup and method

This study aims to disclose the effect of alcohol additions on the droplet combustion characteristics of oleic acid-alcohol fuel blends. The experimental configuration of the present study is illustrated in **Figure 1**. The investigation was performed under atmospheric pressure and normal gravity conditions. A rectangular compartment prevented airflow interference with the droplet during the droplet combustion test [43]. The data collection system comprises a computer, 2 digital cameras, a data logger, and a thermocouple. A self-illuminated direct imaging technique was used to track the temporal evolution of droplet combustion. Several well-known methods, such as suspension, free fall, and heating plate methods, were used to analyze droplet combustion behavior [44]. According to Wang *et al.* [45], the suspension method is simple to generate a droplet under a static condition, which is suitable for measuring droplet parameters such as diameter and temperature. A suspended droplet method was chosen to easily observe the combustion characteristics since the droplet was suspended on the fiber or wire in a fixed position. An R-type thermocouple (Ø200 µm) was used to suspend the droplet and simultaneously measure its temperature. The R-type thermocouple was linked to the Advantech USB-4,718 series data logger, measuring droplet temperature evolution throughout the experiment with a sampling rate of 10 Hz and a maximum error of ± 2.5 ℃. The droplet was generated using a 10 µL microsyringe and suspended on the thermocouple tip. The initial volume of the droplet is 3.05 µL, equivalent to 1.8 ± 0.05 mm of the droplet diameter. Each fuel blend was tested for ten samples to ensure the repeatability of the experiment.

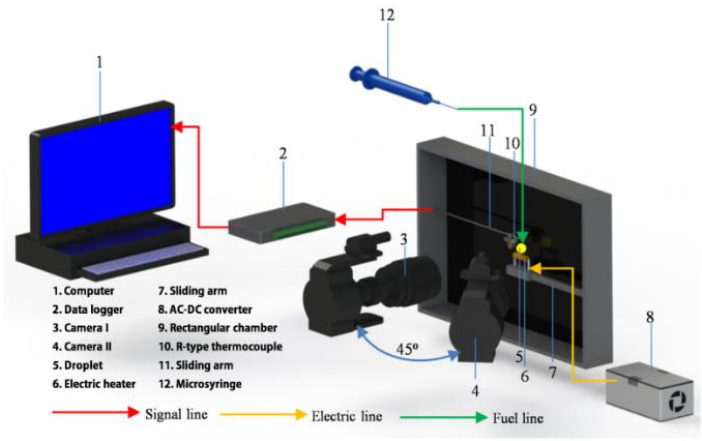

Figure 1 Schematic of the experimental setup.

Two cameras were used to track the temporal evolution of the droplet combustion. Both cameras were recorded at 60 fps with an image resolution of 1,920×1,080 pixels. A Nikon D3400 was used to trace the flame evolution throughout the test with a spatial resolution of 18 pixels/mm. An Olympus E-M5 II as the second camera with a 50 pixels/mm spatial resolution was operated to acquire the droplet dynamic evolution throughout the test. As indicated in **Figure 1**, both cameras were positioned 10 cm away from the droplet. A Ni-Cr wire heater was utilized to heat the droplet, supplied by an electric source of 220 V alternating current converted to 12 V direct current using a step-down transformer. The thermocouple tip was kept 3 mm above the heater to obtain a heating of 720 °C. The transient droplet heating was exposed until the droplet ignited to avoid a heating effect during the test.

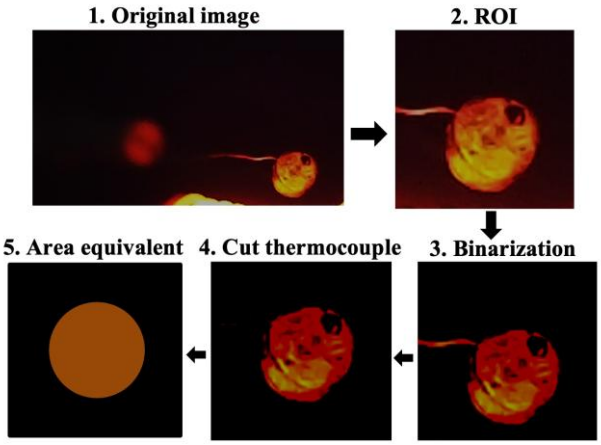

Figure 2 The droplet image processing method.

Droplet image post-processing procedure

The ImageJ software was operated for the post-processing procedure to examine the temporal change of flame dimension and droplet diameter. **Figure 2** depicts the schematic of the droplet image processing procedure derived from earlier studies [15,46,47]. The projected area technique was employed to determine the evolution of droplet diameter. The region of interest (ROI, 300×300 pixels) was extracted from the original image (1,920×1,080 pixels). The droplet boundaries were then separated from their surroundings using the binarization procedure. The thermocouple wire was trimmed and separated from the droplet to obtain the droplet projection region preceding the binarization procedure. The droplet projection area method was used to determine the droplet equivalent diameter with a known spatial resolution (α) of 50 pixels/mm as the reference. The flame height was obtained by calculating the total pixels between the flame tip and the bottom of the non-luminous flame zone. Then, the actual flame height could be acquired using the known spatial resolution α = 18 pixels/mm as the reference.

Results and discussion

The ignition delay time and burning lifetime

The ignition delay time and burning lifetime presented in **Figure 3** were normalized using the squared initial droplet diameter. The ignition delay, often referred to as the transient heating phase, represents the duration from the initial heating of the droplet to the onset of combustion. The use of alcohol as an additive is intended to reduce fuel viscosity and boost fuel volatility, which are 2 main problems when applying biodiesel fuel in spray combustion. With higher volatility, alcohol is faster to form a combustible mixture when exposed to the heat source, which promotes rapid ignition. The OA-M fuel blend exhibits the shortest ignition delay period compared to other fuel blends, and the trend indicates that ignition delay time increases for alcohols with longer carbon chains. The ignition delay period is almost similar between the oleic acid-methanol (OA-M) and oleic acid-ethanol (OA-E) fuel blends. Meanwhile, the oleic acid-propanol (OA-P) fuel blend resembles the oleic acid-butanol (OA-B) fuel blend. From these results, considering the ignition delay time, it is recommended to use ethanol as the fuel blend

rather than methanol. Since the ignition delay period was not too different, a significant difference in energy content between these 2 additives must be considered to obtain higher power generation.

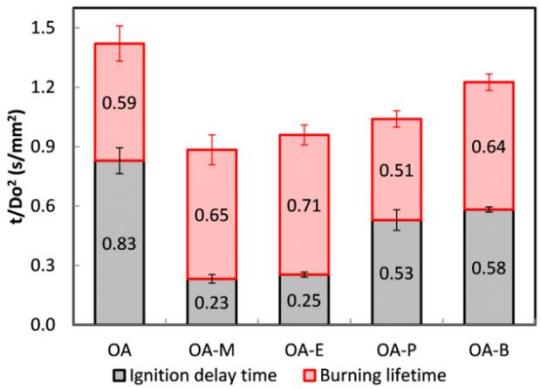

Figure 3 The ignition delay time and burning lifetime.

The burning lifetime is calculated from the initial combustion until the flame extinction. During the combustion process of liquid fuel droplets, partially premixed and diffusion combustion modes occur sequentially throughout the entire process. The combustion process characterized by an extended ignition delay time results in more liquid fuel evaporating and combusting in premixed conditions rather than in diffusion mode, subsequently leading to a reduced burning lifetime. This behavior was proven by the higher flame appearance during the early combustion stage of OA compared to fuel blend combustion due to the vapor accumulation along the heating phase, as shown in **Figure 8**. In contrast, the shorter ignition delay time tends to have a longer burning lifetime. Therefore, OA-P and OA-B fuel blends have a shorter burning lifetime than OA-M and OA-E fuel blends. Compared to OA, only OA-P has a lower burning lifetime, which means 2-propanol can reduce both the partially premixed and diffusion combustion modes of the base fuel. A longer ignition delay encourages the partially premixed flame ignition. The appearance of the yellowish flame indicates the transition into the diffusion combustion mode. The partially premixed flames are closer to the droplets than diffusion flames since the premixed flames formed from fuel vapor accumulation around the droplet [48,49]. During the partially premixed and diffusion combustion modes, a different portion of fuel evaporated between the base fuel and the fuel blend. Considering these 2 modes, it is evident that OA-B exerts the least influence. In contrast, OA-M demonstrates the most substantial effect on decreasing the droplet lifetime or the total ignition delay time and burning lifetime.

Droplet diameter evolution

Figure 4 depicts the progression of droplet diameter throughout the ignition delay period to the flame extinction at the end of the burning lifetime. This graph illustrates the correlation between normalized squared droplet diameter (D^2/D_0^2) and normalized time (t/D_0^2). Based on the droplet diameter evolution behavior, the lifetime of the droplet is categorized into 3 distinct phases for the base fuel and 4 phases for the fuel blends, consisting of the heating (t_1), the microexplosive combustion (t_2), the unsteady combustion (t_3), and the quasi-steady combustion (t_4). During the heating phase, the heating-up process causes the liquid fuel to expand as it absorbs the heat exposed from the heater. When the internal droplet temperature rises and the fuel near the droplet surface reaches its vapor pressure, bubble formation creates a large void space inside the droplet, leading to volumetric expansion [50,51]. At this stage, the volumetric expansion rate of the droplet exceeds the surface evaporation rate of the droplet, which causes the value of D^2/D_0^2 to be increased to exceed 1 for the combustion of all the fuel blends. The magnitude of volumetric expansion is a function of differences in boiling points between fuel blend constituents [52]. Therefore, only slight expansion with a maximum D^2/D_0^2 equal to 1.369 occurs in OA due to the homogeneous species inside the fuel droplet. The

decreasing fuel density due to temperature rise causes the volumetric expansion in OA. Moreover, liquid fuel droplets with high viscosity and surface tension inhibit the movement of the trapped bubble across the droplet surface boundary. The tendency of t_1 is similar between OA and OA-B, while OA-P is similar to OA-E. The highest volumetric expansion occurs in the OA-M fuel blend during the heating phase, reaching a maximum D^2/D_0^2 equal to 5.325.

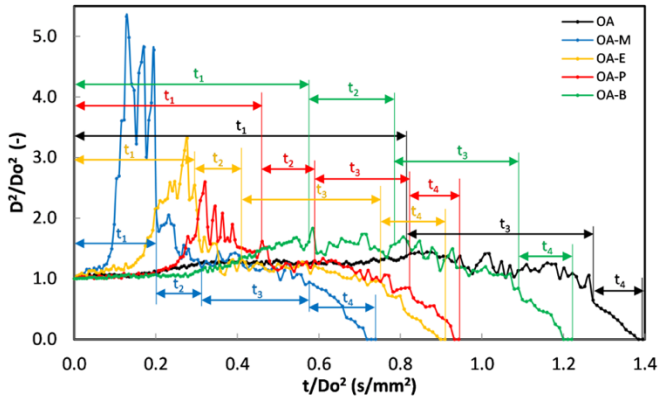

Figure 4 Temporal evolution of normalized squared droplet diameter.

The t_1 ends when the local combustible mixture reaches its ignition point, and a small flame sheet envelops the droplet. Then, the fuel blend enters the microexplosive combustion phase, dominated by alcohol evaporation with a bluish flame during this stage. The microexplosive combustion (t_2) period is extended with the longer carbon chain length of alcohol but with less microburst intensity, as shown in **Figure 7**. The rapid expansion with a larger pre-breakup bubble diameter is related to a higher volatility differential among fuel constituents [53]. Alcohol with less volatility, such as 2-propanol and n-butanol, creates a bubble population with low internal pressure. Therefore, these alcohols have a lower ability to break the high viscous layer of OA, inhibiting the vapor transport with a longer microexplosion delay time. These additives need a higher temperature to ignite, and some amount of OA has been evaporated during the microexplosive combustion phase. The concurrent evaporation processes of the fuel blend constituents generated 2 typical flames around the droplet, consisting of a yellowish flame as the typical flame of OA and a bluish flame as the typical flame of alcohol. The higher volatility alcohols, such as methanol and ethanol, have a shorter t_2 period but more significant droplet size fluctuations. The greater ability of methanol and ethanol to evaporate early when the OA is still in the liquid phase forced the gas phase of alcohol to transport across the droplet interface. This process is very fast, producing high-intensity microbursts and leaving only a few amounts of alcohol when the OA begins to evaporate.

Previous research found that microexplosions occurred during the combustion process of a ternary fuel blend of diesel-biodiesel-ethanol when the alcohol concentration ranged between 10 and 40 vol% [54]. In comparison, the other study mentioned that the strongest microexplosion was obtained when the ethanol portion in biodiesel fuel was 50 % of the fuel blend concentration. Since the microexplosion is closely related to the internal inhomogeneity, the strongest microexplosion occurs when the constituents have equal volumes [12]. In another study on the evaporation process between FAME-ethanol fuel blends, the burning lifetime was reduced when the ethanol content was raised from 20 % to 30 vol% [55]. In the present study, we only used a 20 vol% alcohol concentration to encourage the microexplosion. Too much alcohol will reduce the total amount of energy density, which means that more fuel is needed to generate the same power output with OA combustion.

After the microexplosive combustion ends, only a minor concentration of alcohol remains within the droplet fuel blends, leading to more stable combustion with less droplet size fluctuation during the t_3. The fluctuation is no longer significant at this stage, as only OA combustion occurs with less bubble population

formation. The volumetric expansion and evaporation rates determined the length of the unsteady combustion period. OA combustion as the base fuel has no t_2. Thus, the t_3 occurs directly after the ignition. The droplet combustion transitions into the t_4 as the droplet size diminishes towards the end of combustion, characterized by a linear curve of the normalized squared droplet diameter that adheres to the D^2-law. During this stage, the smaller droplet size has a higher surface-to-volume ratio, which encourages fuel vapor movement toward the droplet interface easier [56]. The fastest mass diffusion rate and sharp droplet size decrement occurred during this stage because the small droplet size instantly evaporates when exposed to high-temperature flames and shortens vapor transport.

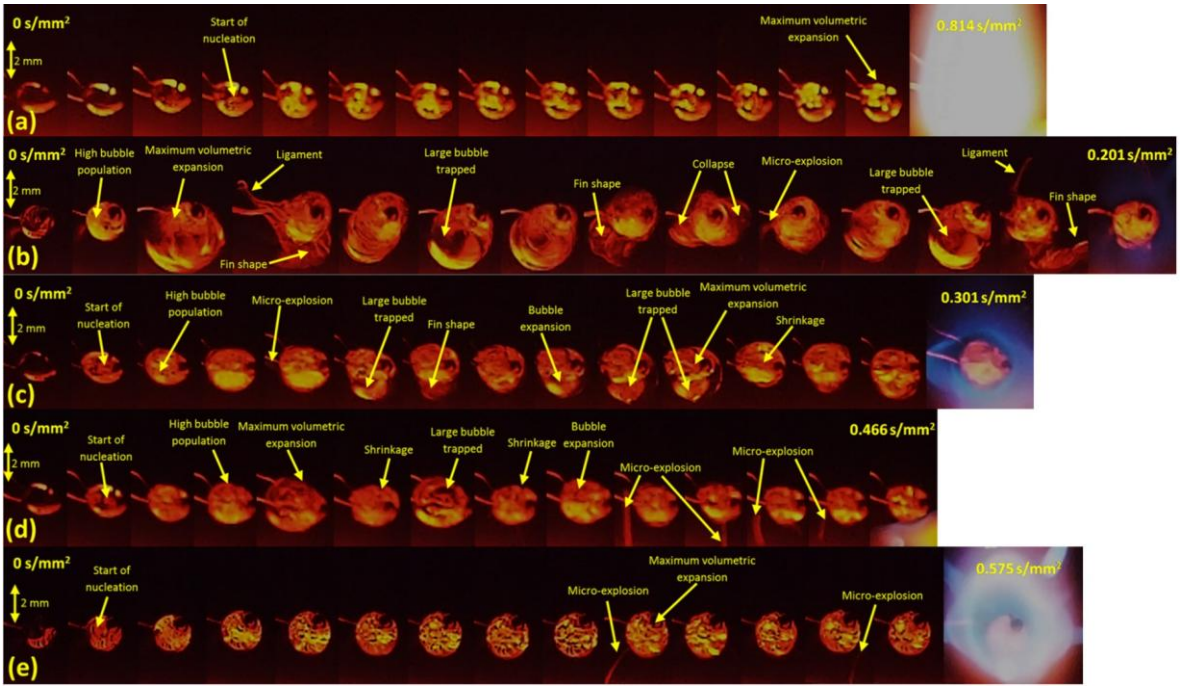

Figure 5 Ignition processes sequence of (a) OA, (b) OA-M, (c) OA-E, (d) OA-P, and (e) OA-B**.**

Figure 5 depicts a sequence of volumetric droplet expansions until it attains ignition temperature. During the heating phase, the boiling process of the alcohol inside the droplet creates many nucleation sites in the form of continuous small bubble growth. The number of active nucleation sites within the droplet determined the bubble population, and adding alcohol to OA accelerates the onset of nucleation. High bubble populations created from active nucleation sites encourage internal circulation due to the different concentrations of gas and liquid phases at the surface and center of the droplet. The high viscosity of OA required high kinetic energy against the internal friction force for the microexplosive breakup because very viscous liquid fuel resists vapor transport toward the droplet surface. The surface tension at the OA interface also inhibits the fuel vapor diffusion across the droplet surface. Microexplosion occurs when the internal pressure from the fuel vapor is sufficient to break the highly viscous interface of OA. In contrast, when the additives have a lower nucleation rate, the bubbles are transported to the droplet surface and diffuse with ambient air at a lower internal pressure without microexplosion.

The value of viscosity and surface tension is a function of temperature, so the heating process during the delay time is also a mechanism to reduce both property values. These processes occur simultaneously, and the abovementioned factors will determine the micro-explosion intensity and strength at the onset of the burning period. One of the most promising applications of secondary atomization technology is the fragmentation of fuel droplets into many small droplets [57]. Microexplosion is an important phenomenon that occurs in binary liquid fuel droplet combustion. Microexplosion causes the droplet diameter to diminish rapidly through child droplet ejection when the bubble

ruptures, leading to a higher burning rate than the combustion without the microexplosion.

The OA combustion starts to burn at the normalized time of 0.814 s/mm^2, and adding alcohol shortens the ignition point around 0.201 - 0.575 s/mm^2. Droplet diameter evolution of OA-M, OA-E, and OA-P fuel blends has a similar tendency toward large volumetric expansion and droplet diameter fluctuation during the heating phase because the evaporation process produces homogeneous nucleation with large and high bubble mobility. In contrast, the highest volumetric expansion with a greater fluctuation for OA-B occurs during the microexplosive combustion phase after reaching the ignition point, as indicated in **Figure 4**. During the heating phase of the OA-B, a high bubble population with smaller bubble sizes occurs due to heterogeneous nucleation. The nucleation mode differences and the number of bubble growths within the liquid fuel droplet depend on the distinction between the boiling points of alcohol and OA as a base fuel. The most severe droplet fragmentation from the parent droplet occurs when methanol is used as an additive since it has the lowest boiling point. The fuel vapor mass flux away from the droplet interface is slower than the heat flux to the droplet from the heater, leading to the bubbles accumulation within the droplet region.

The alcohol vapor trapped inside the droplet at high vapor pressure causes a significant droplet volumetric expansion. This mechanism is essential since the greater droplet volume increases the total droplet surface area, which is the region where the fuel vapor diffuses with the surrounding air. Thus, the fuel reaction zone with ambient air is enlarged, increasing the thermal absorption with a higher evaporation rate and decreasing the ignition time. The trapped bubble inside the droplet expands continuously as numerous small bubbles merge to create a few larger bubbles. Fuel droplet constituents with high volatility disparities encourage the coalescence of several microbubbles into larger vapor bubbles [58]. The bubble coalescence is a precursor to increased local internal pressure in the droplet. The different bubble formations and nucleation modes within the droplet then distinguish the droplet breakup structure.

The droplet rupture creates a ligament detachment and fin shape, with more liquid fuel involved during the droplet ejection in OA-M. The fin shape also appears in OA-E combustion but with a smaller structure due to the weaker microexplosion strength. The ligament and fin shape structure are subsequent behaviors following a large bubble trapped within the droplet. The previous study stated that large bubbles trapped within the droplet are caused by a large surface tension of the base fuel [43]. In the present study, OA with a high surface tension inhibits the high-volatility alcohol vapor from transporting across the droplet interface. OA-E and OA-P have continuous bubble expansion and droplet shrinkage due to nucleation and growth, trapped bubbles, and child droplets detaching from the parent droplet interface. Unlike other alcohol additives, child droplet ejection in OA-B does not cause significant shrinkage. It only creates a thin microburst ejection structure, which involves less bulk of liquid fuel. The n-butanol vaporization forms small bubble sizes with low internal pressure. The vapor phase is ejected from the parent droplet at a higher temperature and only creates a thin droplet breakup.

Droplet combustion temperature

The combustion temperature indicates the total energy released during combustion [59]. **Figure 6** depicts the progression of droplet temperature and its first derivative throughout the test. The first-derivative curve of the droplet temperature was derived using the first-order backward differencing scheme approximation. In the experiment, 3 peaks were identified for the OA combustion, whereas only 2 peaks were observed for the fuel blend combustion. During the heating of OA combustion, the initial peak of the first derivative curve is followed by a constant low value as the droplet temperature rises until it attains the boiling point. Then, it continues by droplet evaporation at a relatively constant temperature, indicating the latent heating regime. Meanwhile, due to its low boiling point temperature, the OA-M fuel blend immediately evaporates from the initial heating.

The second peak in OA and the first peak in fuel blends occur around the ignition point, which is continued by the flame appearance that raises the droplet temperature significantly. Oxygenated additives can accelerate the local combustible mixture formation, increasing ignition probability and decreasing ignition delay with a lower ignition temperature. The overall oxygen content within fuel additives determines the

degree of effectiveness during combustion [40]. Short-chain alcohols, such as methanol and ethanol, are easier to attain local combustible mixtures and are more reactive due to higher oxygen concentrations, promoting an earlier ignition. The combustible mixture formation is enhanced when the liquid fuel is atomized into many smaller droplets through a microexplosion mechanism [60]. The microexplosive combustion in fuel blends is dominated by alcohol decomposition, resulting in a high-temperature increase tendency related to the transition from the evaporation stages to the beginning of the combustion stages with rapid evaporation rates. Although alcohol has a lower energy content than OA as a base fuel, the higher burning rate of alcohol than OA diminishes the lower energy content, resulting in a significant increase in droplet temperature.

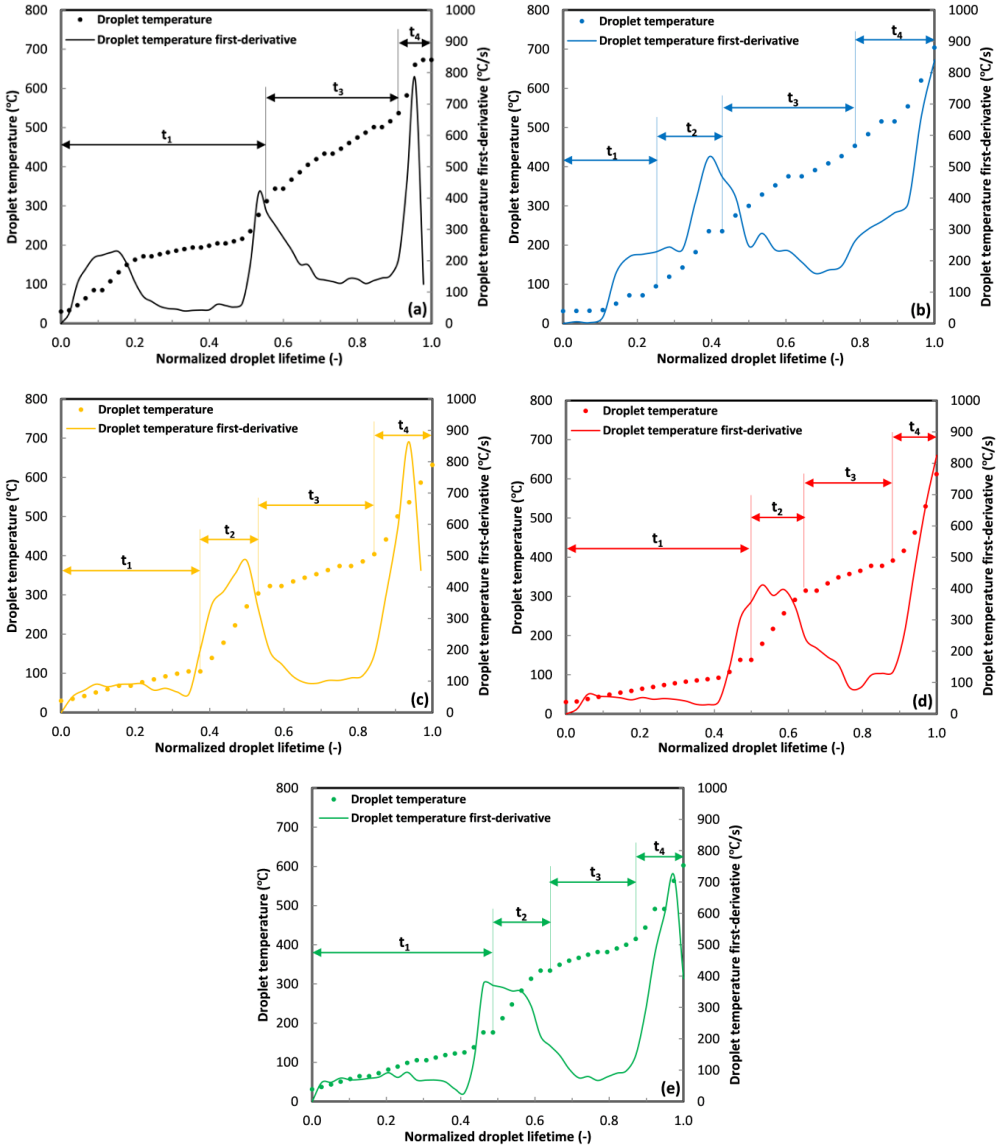

Figure 6 Temporal evolution of droplet temperature and droplet temperature first-derivative of (a) OA, (b) OA-M, (c) OA-E, (d) OA-P, and (e) OA-B combustion.

The droplet temperature tendency at the t_3 stage experiences an insignificant increase with an almost constant first-derivative profile between 2 peaks associated with the base fuel evaporation. The droplet diameter expands and shrinks continuously during this stage without significant droplet size reduction. The transition from the t_3 to the t_4 phase with a small droplet size is the onset of the droplet peak temperature. The rapid combustion process occurs at this stage, resulting in a high temperature of combustion products.

Combustion ends when the liquid fuel droplet has completely evaporated, and the flame sustains for a while before extinction due to the remaining fuel vapor accumulation. Direct contact between the flame and the thermocouple tip produces the droplet peak temperature in combustion as the final peak of the first derivative curve.

The disadvantage of utilizing alcohol additives is related to the lower energy density compared to OA. The fuel blend has a lower overall energy content because it contains oxygenated compounds, suggesting that more fuel is needed to deliver the same power generation. However, OA-M has a higher droplet peak temperature than OA at the end of combustion, even though it has a lower energy density. In addition to the rise in oxygen content and volatility of the fuel blends, the higher droplet peak temperature of OA-M compared to OA is attributable to a greater fuel consumption rate associated with the lower density and viscosity of methanol as an oxygenated compound. Higher oxygen content in a liquid fuel droplet encourages more complete combustion and faster combustion [61].

Flame visualization and evolution

Flame visualization qualitatively analyzes the droplet combustion behavior. During the microexplosive combustion (t_2), each fuel blend has a typical microexplosion flame that distinguishes it from each other, as shown in **Figure 7**. At this stage, microexplosion is observed as a microburst flame because the child droplets from the parent droplet have direct contact with the primary flame before forming an elongated microflame structure. The OA-M blend produces a robust microexplosion with numerous child droplet ejections around the primary flame. The microexplosion intensity is diminished for a longer carbon-chain alcohol by only producing several child droplet ejections. A higher possibility of microexplosion was obtained when introducing low-boiling alcohol to the base fuel with much lower volatility [23].

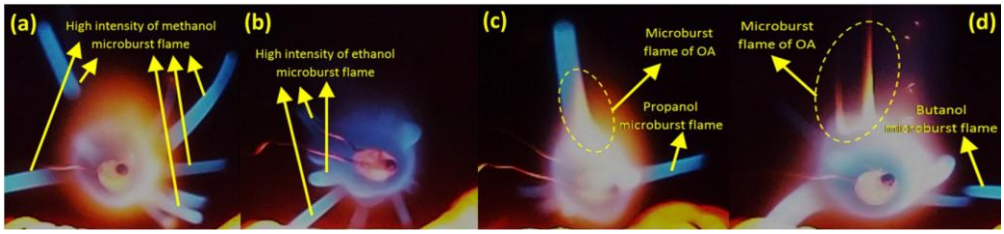

Figure 7 Typical microexplosion flame of (a) OA-M, (b) OA-E, (c) OA-P, and (d) OA-B.

The microexplosive combustion in OA-B combustion occurs at a higher temperature because it has the longest microexplosion delay time. It allows some portion of OA as a base fuel to evaporate and eject along with the vapor from n-butanol. This simultaneous process then produces a yellowish microburst flame from the burning of OA and a bluish n-butanol flame. This behavior also appeared in OA-P combustion, which was observed to merge with the microburst flame of 2-propanol (**Figure 7(c)**) but did not appear in OA-M and OA-E combustion. The previous study revealed this behavior and found that fewer differences in boiling points among the fuel blend constituents would encourage more base fuel fraction to evaporate and burn during the microexplosive combustion [62].

Figure 8 depicts the evolution of flame height determined by calculating the total pixels between the flame tip and the bottom of the non-luminous flame zone. This graph was presented in the normalized flame evolution as the instantaneous ratio between the flame height and initial droplet diameter. Analysis of the flame evolution behavior is essential since it is associated with a few parameters, such as soot formation, combustion stages, and flame standoff ratio. The flame fluctuation during the t_2 phase is associated with the microburst flame from the ejected child droplet. As a base fuel, OA exhibits a more rapid growth rate in flame size than blended fuel during the initial combustion phase, attributed to the greater accumulation of fuel vapor at the ignition point.

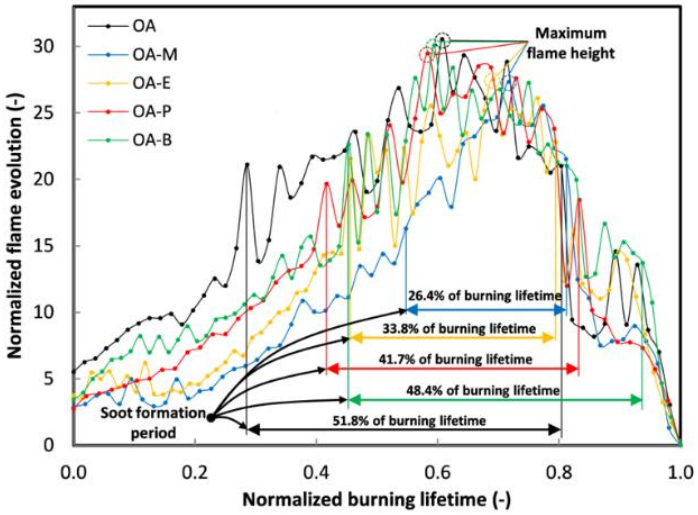

Figure 8 Flame evolution during droplet combustion.

The high oxygen content in methanol, about 49.93 wt%, causes OA-M to form a combustible mixture quickly in a narrow fuel reaction zone around the droplet, resulting in shorter flame dimensions during the t_2 phase. Meanwhile, the lower oxygen concentration in n-butanol, about 21.58 wt%, causes the fuel vapor to require more oxygen from the air and diffuse at a wider distance from the droplet due to the influence of natural convection to form a local combustible mixture. Besides the lower oxygen concentration, the greater flame dimensions in OA-P and OA-B compared to OA-M and OA-E are attributable to the simultaneous combustion of the alcohol with some portion of OA due to the higher ignition points of 2-propanol and n-butanol. After most alcohol fractions burned, the non-luminous flame zone encircling the droplet became brighter. The flame luminosity was initially faint during the first flame appearance when alcohol was burned, but it transitioned to a bright flame luminosity when the base fuel was burned. Then, the bright flame is followed by soot aggregate and soot spread [63]. The gradual transformation of the blue flame into a yellowish flame denotes the beginning of soot growth. The appearance and intensity of the yellowish flame depend on the soot formation inside the flame sheet [64]. Normal gravity experiments of droplet combustion always generate soot emissions that blow away due to natural convection. Soot formation appears at the flame tip on unsaturated molecules like OA, which creates a higher flame dimension [23,65]. This behavior promotes the highest flame dimension of OA combustion compared to the fuel blends.

The different flame shapes between the base fuel and fuel blends are related to variations in combustible mixture formation, heat transfer by natural convection, gas density, and soot formation. OA combustion generates a high temperature from the onset of combustion. As the temperature rises, the gas density decreases, resulting in a larger flame dimension due to natural convection [66]. Thus, an elongated flame structure appears during the unsteady combustion phase rather than the microexplosive combustion phase of alcohol combustion. Oxygen as an oxidizing agent improves combustion performance with a faster combustion rate and suppresses soot formation. Therefore, less soot was produced as the higher proportion of an oxygenated component within the fuel blend. Methanol has the most significant effect in delaying the onset of soot accumulation observed on the flame tip. The soot formation at the flame tip of OA-M combustion begins to appear at 54.7 % of the burning lifetime and only sustains about 26.4 % of the burning lifetime. Meanwhile, n-butanol, with the least oxygen content, starts the soot accumulation at 45.3 % of the burning lifetime and sustains it through 48.4 % of the burning lifetime. OA combustion started the soot accumulation early at 28.6 % of the burning lifetime and has the longest period of about half of the combustion time.

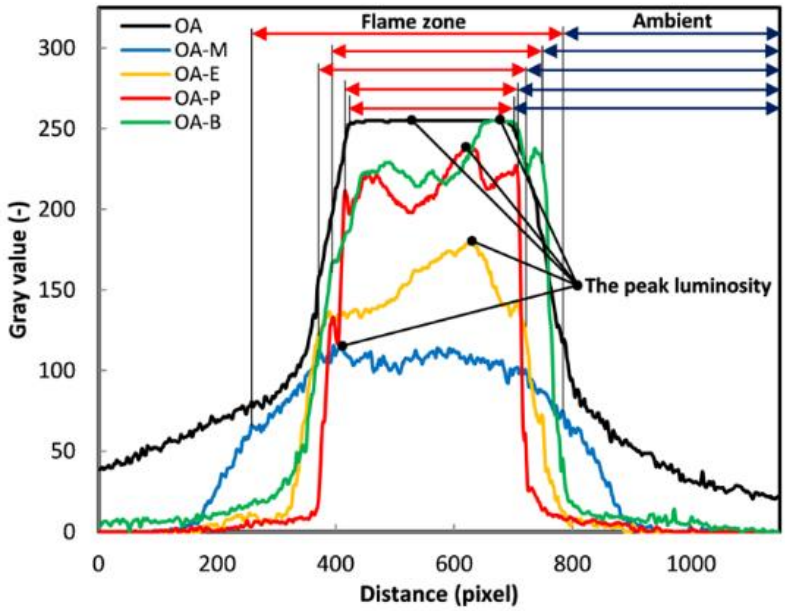

Figure 9 Flame luminosity profile.

Analyzing the flame dimension and area, soot precursor species formation, and flame luminosity are all possible methods for determining soot formation without directly measuring soot fractions [40]. **Figure 9** depicts the flame luminosity profile along the horizontal trajectory intersecting the flame structure during the initial combustion stage, or the t_3 phase for the base fuel and the t_2 phase for the fuel blends. The gray value characterizes the soot generation propensity, which is closely related to flame luminosity. A higher gray value of OA combustion denotes that more soot particles are formed. A shorter alcohol-carbon chain structure elevates oxygen availability in the fuel blends, facilitating complete combustion with lower soot particles, indicated by a blue flame in the non-luminous flame zone around the droplet with lower luminosity. Due to its abundant oxygen content, methanol is the most effective alcohol for suppressing the soot generation propensity, reducing the peak luminosity and average value along the flame zone. N-butanol has the least impact and the same peak luminosity as OA, but it still has a lower average gray value than OA combustion. OA combustion has the highest gray value of the ambient region, indicating that the enormous radiation emitted from the combustion process reaches an extensive area outside the flame zone.

The flame standoff ratio (FSR) is described as the ratio between the instantaneous flame diameter (D_f) and the instantaneous droplet diameter (D). In the droplet experiment under normal gravity with a large enough droplet size, a spherical flame is not formed due to the influence of the buoyancy effect and natural convection. Thus, as in several previous studies, the outermost boundary of the luminous flame zone along the horizontal axis is regarded as the flame diameter [67,68]. The FSR is commonly recognized as the primary indicator for evaluating the flame diffusion behavior in droplet combustion and surface phenomena related to Stefan flux [69,70]. Stefan flux is related to mass diffusion, which forces the flame away from the droplets when the evaporation rate is high. The FSR curve is divided into 2 regions for base fuel combustion and 3 regions for fuel blend combustion, as shown in **Figure 10**. The average FSR values of OA, OA-M, OA-E, OA-P, and OA-B were 3.64, 4.06, 3.79, 3.77, and 3.73, respectively.

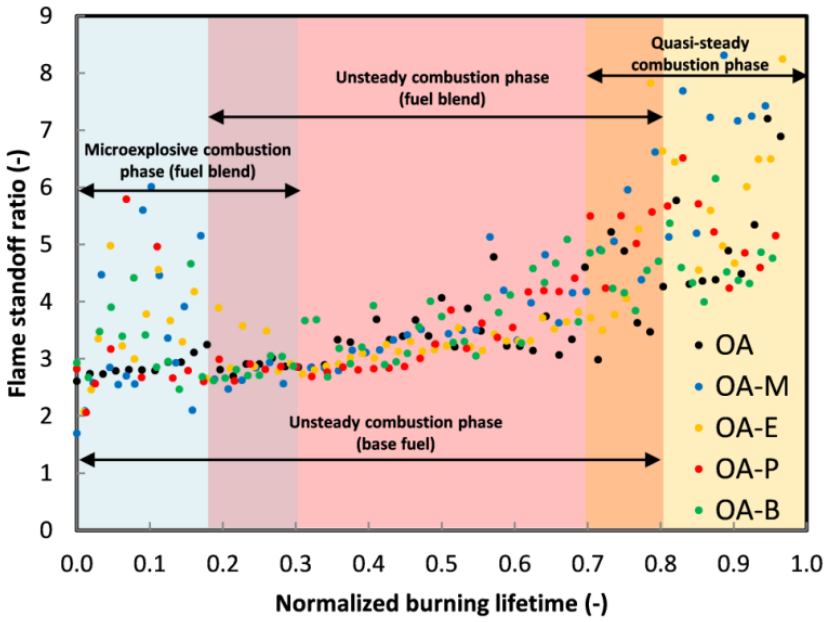

Figure 10 Flame standoff ratio.

The addition of alcohol to OA increases the vapor pressure of the fuel blends with a large evaporation rate, particularly during the microexplosion phase, which ends at 18 - 31 % of the burning lifetime. Microexplosion causes a fluctuating flame diameter evolution during the onset of combustion, leading to an increase in the FSR value. Therefore, OA has the lowest average FSR, while OA-M, with the fastest evaporation rate, has the highest average FSR. After the microexplosion, the unsteady combustion phase of the fuel blend produces a relatively constant FSR with low fluctuations. The FSR of oleic acid and its mixture is inconsistent with the FSR based on the D^2-law, which has a constant value. Several other investigations, including Wang *et al.* [71]; Singh *et al.* [72]; Setyawan *et al.* [73], also obtained similar results. FSR increases with combustion time due to the influence of fuel vapor accumulation, especially after reaching 70 - 80 % of the burning lifetime when it enters the quasi-steady combustion phase with relatively small droplet sizes. The reduced droplet size increases the surface area-to-volume ratio, accelerating the fuel vapor diffusion rate. This phenomenon aligns with research by Liu *et al.* [74], which resulted in a higher FSR with a smaller initial droplet diameter.

Conclusions

This study investigated the single isolated droplet combustion behavior and mechanism of oleic acid as the surrogate compound of vegetable oil with alcohol additives. The study employed the suspended droplet technique supported by a self-illuminated direct imaging procedure. The alcohol additives improve the combustion behavior, which depends on different properties among the fuel blend constituents. The ignition delay depends on fuel volatility, with methanol addition resulting in the shortest heating phase period because it has the highest boiling point difference with the base fuel. While all the fuel blends reduce the droplet lifetime compared to the OA combustion, only OA-P combustion shortens the burning lifetime period among the fuel blends. The volumetric expansion of OA-M combustion exhibited the highest maximum D^2/D_0^2 value of 5.325. The microexplosive combustion phase is prolonged for the fuel blend with less alcohol volatility because the bubble population with a low internal pressure has a smaller ability to break the high viscous layer of the OA interface. Bubble coalescence served as a precursor to increased local internal pressure, and the different droplet breakup structures depend on the bubble formation and nucleation mode. The OA-M combustion has the highest droplet peak temperature, although it has a lower energy content. The different boiling points between OA and alcohols distinguish the

typical microexplosion flame. The alcohol additives effectively diminish the sooting propensity and delay the onset of soot accumulation. OA-M has the highest average FSR values due to the microexplosive behavior and faster evaporation rate. These experimental findings provide a reference for further studies on the microexplosion mechanism associated with alcohol additives to enhance the combustion performance of viscous fuels such as vegetable oil or biodiesel fuel for application in internal combustion engines.

Acknowledgements

This work was supported by Faculty of Engineering, Brawijaya University, Indonesia (DIPA Research Group: Grant number: 119/UN10.F07/PN/2024).

References

[1] J Han, LMT Somers, R Cracknell, A Joedicke, R Wardle and VRR Mohan. Experimental investigation of ethanol/diesel dual-fuel combustion in a heavy-duty diesel engine. *Fuel* 2020; **275**, 117867.

[2] W Shang, J Cao, S Yang and Z He. In-flame soot quantification of N-Hexadecane droplets using diffused back-illumination extinction imaging. *Case Studies in Thermal Engineering* 2022; **30**, 101699.

[3] Y Zhang, R Huang, Y Huang, S Huang, Y Ma, S Xu and P Zhou. Effect of ambient temperature on the puffing characteristics of single butanol-hexadecane droplet. *Energy* 2018; **145**, 430-441.

[4] D Nurmukan, MV Tran, YM Hung, G Scribano and CT Chong. Effect of multi-walled carbon nanotubes on pre-vaporized palm oil biodiesel/air premixed flames. *Fuel Communications* 2021; **8**, 100020.

[5] N Jeyakumar, B Narayanasamy, D Balasubramanian and K Viswanathan. Characterization and effect of *Moringa Oleifera Lam*. antioxidant additive on the storage stability of Jatropha biodiesel. *Fuel* 2020; **281**, 118614.

[6] M Lapuerta, JJ Hernandez, D Fernandez-Rodriguez and A Cova-Bonillo. Autoignition of blends of n-butanol and ethanol with diesel or biodiesel fuels in a constant-volume combustion chamber. *Energy* 2016; **118**, 613-621.

[7] M Plank, G Wachtmeister, E Remmele, K Thuneke and P Emberger. Ignition characteristics of straight vegetable oils in relation to combustion and injection parameters, as well as their fatty acid composition. *Fuel Processing Technology* 2017; **167**, 271-280.

[8] M ElKelawy, HA Bastawissi, EA El-Shenawy, H Panchal, K Sadashivuni, D Ponnamma, M Al-Hofy, N Thakar and R Walvekar. Experimental investigations on spray flames and emissions analysis of diesel and diesel/biodiesel blends for combustion in oxy-fuel burner. *Asia-Pacific Journal of Chemical Engineering* 2019; **14(6)**, e2375.

[9] EG Giakoumis. Analysis of 22 vegetable oils' physico-chemical properties and fatty acid composition on a statistical basis, and correlation with the degree of unsaturation. *Renewable Energy* 2018; **126**, 403-419.

[10] E Marlina, W Wijayanti, L Yuliati and ING Wardana. The role of pole and molecular geometry of fatty acids in vegetable oils droplet on ignition and boiling characteristics. *Renewable Energy* 2020; **145**, 596-603.

[11] D Qi, W Xing, P Luo, J Liu and R Chen. Effect of alcohols on combustion characteristics and particle size distribution of a diesel engine fueled with diesel-castor oil blended fuel. *Asia-Pacific Journal of Chemical Engineering* 2020; **15(4)**, e2477.

[12] C Chao, H Tsai, K Pan and C Hsieh. On the microexplosion mechanisms of burning droplets blended with biodiesel and alcohol. *Combustion and Flame* 2019; **205**, 397-406.

[13] H Zhang, Z Wang, Y He, J Huang and K Cen. Interactive effects in 2-droplets combustion of RP-3 kerosene under sub-atmospheric pressure. *Processes* 2021; **9(7)**, 1229.

[14] J Wang, X Huang, X Qiao, D Ju and C Sun. Experimental study on evaporation characteristics of single and multiple fuel droplets. *Journal of the Energy Institute* 2020; **93(4)**, 1473-1480.

[15] L Wang, J Wang, X Qiao, D Ju and Z Lin. Effect of ambient temperature on the micro-explosion characteristics of soybean oil droplet: The phenomenon of evaporation induced vapor cloud. *International Journal of Heat and Mass Transfer*

2019; **139**, 736-746.

[16] M Mikami, N Motomatsu, K Nagata, Y Yoshida and T Seo. Flame spread between 2 droplets of different diameter in microgravity. *Combustion and Flame* 2018; **193**, 76-82.

[17] M Mikami, K Matsumoto, Y Yoshida, M Kikuchi and DL Dietrich. Space-based microgravity experiments on flame spread over randomly distributed n-decane-droplet clouds: Anomalous behavior in flame spread. *Proceedings of the Combustion Institute* 2021; **38(2)**, 3167-3174.

[18] AP Pinheiro, JM Vedovoto, AS Neto and BGM Wachem. Ethanol droplet evaporation: Effects of ambient temperature, pressure and fuel vapor concentration. *International Journal of Heat and Mass Transfer* 2019; **143**, 118472.

[19] K Pandey and S Basu. High vapour pressure nanofuel droplet combustion and heat transfer: Insights into droplet burning time scale, secondary atomisation and coupling of droplet deformations and heat release. *Combustion and Flame* 2019; **209**, 167-179.

[20] EN Rose, V Nayagam, DL Dietrich, MC Hicks, UG Hegde, RE Padilla and FA Williams. Autoignition dynamics of n-dodecane droplets under normal gravity. *Combustion Science and Technology* 2020; **194(9)**, 1830-1849.

[21] HY Setyawan and M Zhu. Cenosphere formation and combustion characteristics of single droplets of vacuum residual oils. *Combustion Science and Technology* 2023; **197(1)**, 59-76.

[22] Y Zhang, R Huang, Z Wang, S Xu, S Huang and Y Ma. Experimental study on puffing characteristics of biodiesel-butanol droplet. *Fuel* 2016; **191**, 454-462.

[23] K Pan and M Chiu. Droplet combustion of blended fuels with alcohol and biodiesel/diesel in microgravity condition. *Fuel* 2013; **113**, 757-765.

[24] K Meng, Y Wu, Q Lin, F Shan, W Fu and K Zhou. Microexplosion and ignition of biodiesel/ethanol blends droplets in oxygenated hot co-flow. *Journal of the Energy Institute* 2019; **92**, 1527-1536.

[25] J Wang, X Qiao, D Ju, L Wang and C Sun. Experimental study on the evaporation and micro-explosion characteristics of nanofuel droplet at dilute concentrations. *Energy* 2019; **183(9)**, 149-159.

[26] MR Chow, JB Ooi, KM Chee, CH Pun, MV Tran, JCK Leong and S Lim. Effects of ethanol on the evaporation and burning characteristics of palm-oil based biodiesel droplet. *Journal of the Energy Institute* 2021; **98**, 35-43.

[27] X Wang, M Dai, J Yan, C Chen, G Jiang and J. Zhang. Experimental investigation on the evaporation and micro-explosion mechanism of jatropha vegetable oil (JVO) droplets. *Fuel* 2019; **258**, 115941.

[28] ING Wardana. Combustion characteristics of jatropha oil droplet at various oil temperatures. *Fuel* 2010; **89(3)**, 659-664.

[29] P Muanruksa and P Kaewkannetra. Combination of fatty acids extraction and enzymatic esterification for biodiesel production using sludge palm oil as a low-cost substrate. *Renewable Energy* 2020; **146**, 901-906.

[30] SK Hoekman, A Broch, C Robbins, E Ceniceros and M Natarajan. Review of biodiesel composition, properties, and specifications. *Renewable and Sustainable Energy Reviews* 2012; **16(1)**, 143-169.

[31] A Gopinath, K Sairam, R Velraj and G Kumaresan. Effects of the properties and the structural configurations of fatty acid methyl esters on the properties of biodiesel fuel: A review. *Journal of Automobile Engineering* 2014; **229(3)**, 357-390.

[32] G Knothe and LF Razon. Biodiesel fuels. *Progress in Energy and Combustion Science* 2017; **58**, 36-59.

[33] N Meiri, P Berman, LA Colnago, TB Moraes, C Linder and Z Wiesman. Liquid-phase characterization of molecular interactions in polyunsaturated and n-fatty acid methyl esters by 1H low-field nuclear magnetic resonance. *Biotechnology for Biofuels* 2015; **8(1)**, 96.

[34] RD Misra and MS Murthy. Straight vegetable oils usage in a compression ignition engine - a review. *Renewable and Sustainable Energy Reviews* 2010; **14(9)**, 3005-3013.

[35] S Xue, K Hou, Z Zhang, H Liu, C Zhu, X Liu and M He. General models for prediction densities and viscosities of saturated and unsaturated fatty acid esters. *Journal of Molecular Liquids* 2021;

341, 117374.

[36] LF Ramírez-Verduzco, JE Rodríguez-Rodríguez and ADR Jaramillo-Jacob. Predicting cetane number, kinematic viscosity, density and higher heating value of biodiesel from its fatty acid methyl ester composition. *Fuel* 2012; **91(1)**, 102-111.

[37] E Torres-Jimenez, MS Jerman, A Gregorc, I Lisec, MP Dorado and B Kegl. Physical and chemical properties of ethanol-diesel fuel blends. *Fuel* 2011; **90(2)**, 795-802.

[38] AI EL-Seesy, Z He and H Kosaka. Combustion and emission characteristics of a common rail diesel engine run with n-heptanol-methyl oleate mixtures. *Energy* 2021; **214**, 118972.

[39] CK Westbrook, CV Naik, O Herbinet, WJ Pitz, M Mehl, SM Sarathy and HJ Curran. Detailed chemical kinetic reaction mechanisms for soy and rapeseed biodiesel fuels. *Combustion and Flame* 2011; **158(4)**, 742-755.

[40] CC Lee, MV Tran, BT Tan, G Scribano and CT Chong. A comprehensive review on the effects of additives on fundamental combustion characteristics and pollutant formation of biodiesel and ethanol. *Fuel* 2021; **288**, 119749.

[41] B Waluyo, M Setiyo, S Saifudin and ING Wardana. Fuel performance for stable homogeneous gasoline-methanol-ethanol blends. *Fuel* 2021; **294**, 120565.

[42] E Sukjit, JM Herreros, KD Dearn, R García-contreras and A Tsolakis. The effect of the addition of individual methyl esters on the combustion and emissions of ethanol and butanol-diesel blends. *Energy* 2012; **42(1)**, 364-374.

[43] E Marlina, W Wijayanti, L Yuliati and ING Wardana. The role of 1.8-cineole addition on the change in triglyceride geometry and combustion characteristics of vegetable oils droplets. *Fuel* 2021; **314**, 122721.

[44] K Meng, L Bao, Y Shi, K Han, Q Lin and C Wang. Experimental investigation on ignition, combustion and micro-explosion of RP-3, biodiesel and ethanol blended droplets. *Applied Thermal Engineering* 2020; **178**, 115649.

[45] Z Wang, B Yuan, Y Huang, J Cao, Y Wang and X Cheng. Progress in experimental investigations on evaporation characteristics of a fuel droplet. *Fuel Processing Technology* 2022; **231**, 107243.

[46] K Han, Y Liu, C Wang, J Tian, Z Song, Q Lin and K Meng. Experimental study on the evaporation characteristics of biodiesel-ABE blended droplets. *Energy* 2021; **236**, 121453.

[47] X Wang, M Dai, J Wang, Y Xie, G Ren and G Jiang. Effect of ceria concentration on the evaporation characteristics of diesel fuel droplets. *Fuel* 2019; **236**, 1577-1585.

[48] A Kumar, HW Chen and S Yang. Diffusion and its effects on soot production in the combustion of emulsified and nonemulsified fuel droplets. *Energy* 2023; **267**, 126521.

[49] IA Ibadurrohman, N Hamidi, L Yuliati and W Winarto. Droplet combustion behavior of methyl oleate-methyl palmitate fuel blend as the surrogate compounds of palm oil biodiesel. *AIP Conference Proceedings* 2024; **3090(1)**, 020002.

[50] DV Antonov, GS Nyashina, RM Fedorenko and AS Filatova. Microexplosive atomization of heterogeneous fuel drops for intensifying their ignition. *Chemical and Petroleum Engineering* 2019; **55(7-8)**, 619-626.

[51] HY Nanlohy, ING Wardana, N Hamidi, L Yuliati and T Ueda. The effect of Rh^{3+} catalyst on the combustion characteristics of crude vegetable oil droplets. *Fuel* 2018; **220**, 220-232.

[52] M Amsal, MV Tran, YM Hung and G Scribano. Experimental study of evaporation of palm biodiesel with multi-walled carbon nanotubes additives at elevated temperatures. *International Journal of Environmental Science and Technology* 2022; **19(7)**, 6611-6624.

[53] DCK Rao, S Syam, S Karmakar and R Joarder. Experimental investigations on nucleation, bubble growth, and micro-explosion characteristics during the combustion of ethanol/Jet A-1 fuel droplets. *Experimental Thermal and Fluid Science* 2016; **89(1)**, 284-294.

[54] MM Avulapati, LC Ganippa, J Xia and A Megaritis. Puffing and micro-explosion of diesel-biodiesel-ethanol blends. *Fuel* 2016; **166**, 59-66.

[55] X Wang, G Wang, L Wang, J Zhang and J Yan. Ethanol evaporation characteristics of the blends of fatty acid methyl ester and ethanol. *Journal of Shanghai Jiaotong University* 2021; **26(2)**, 210-217.

[56] N Hamidi, IA Ibadurrohman, L Yuliati, W Winarto and DB Darmadi. The effect of alcohol compounds on droplet combustion characteristics of unsaturated fatty acid of linoleic acid. *Trends in Sciences* 2023; **20(7)**, 6720.

[57] DV Antonov, GV Kuznetsov, PA Strizhak and RM Fedorenko. Micro-explosion of droplets containing liquids with different viscosity, interfacial and surface tension. *Chemical Engineering Research and Design* 2020; **158**, 129-147.

[58] DCK Rao and S Karmakar. Crown formation and atomization in burning multi-component fuel droplets. *Experimental Thermal and Fluid Science* 2018; **98**, 303-308.

[59] N Hamidi and J Nugroho. Single droplet combustion characteristics of petroleum diesel-philippine tung biodiesel blends. *Trends in Sciences* 2021; **18(24)**, 1409.

[60] X Huang, J Wang, Y Wang, X Qiao, D Ju, C Sun and Q Zhang. Experimental study on evaporation and micro-explosion characteristics of biodiesel/n-propanol blended droplet. *Energy* 2020; **205**, 118031.

[61] JB Ooi, JH Yap, MV Tran and JCK Leong. Experimental investigation on the droplet burning behavior of diesel-palm biodiesel blends. *Energy and Fuels* 2019; **33(11)**, 11804-11811.

[62] IA Ibadurrohman, N Hamidi, L Yuliati, W Winarto and M Mikami. The impact of ethanol addition on the droplet combustion mechanism of saturated and unsaturated fatty acid/fatty acid methyl ester molecules. *Fuel* 2023; **334**, 126731.

[63] Y Zhang, R Huang, Y Huang, S Huang, P Zhou, X Chen and T Qin. Experimental study on combustion characteristics of an n-butanol-biodiesel droplet. *Energy* 2018; **160**, 490-499.

[64] S Parag and V Raghavan. Experimental investigation of burning rates of pure ethanol and ethanol blended fuels. *Combustion and Flame* 2009; **156(5)**, 997-1005.

[65] IA Ibadurrohman, N Hamidi and L Yuliati. The role of the unsaturation degree on the droplet combustion characteristics of fatty acid methyl ester. *Alexandria Engineering Journal* 2022; **61(3)**, 2046-2060.

[66] IA Ibadurrohman, N Hamidi, L Yuliati and BA Valentino. Experimental investigation on the effect of carbon chain length to the droplet combustion characteristic of fatty acid methyl ester. *IOP Conference Series: Materials Science and Engineering* 2021; **1034**, 012060.

[67] H Zhang, Z Wang, Y He, J Xia, J Zhang, H Zhao and K Cen. Ignition, puffing and sooting characteristics of kerosene droplet combustion under sub-atmospheric pressure. *Fuel* 2021; **285**, 119182.

[68] Á Muelas, P Remacha and J Ballester. Droplet combustion and sooting characteristics of UCO biodiesel, heating oil and their mixtures under realistic conditions. *Combustion and Flame* 2019; **203**, 190-203.

[69] Y Zhong, J Xu, Y Pan, Z Yin, X Wang, Y Zhou and Q Huang. Combustion characteristics of aromatic-enriched oil droplets produced by pyrolyzing unrecyclable waste tire rubber. *Fuel Processing Technology* 2022; **226**, 107093.

[70] G Singh, M Esmaeilpour and A Ratner. Effect of carbon-based nanoparticles on the ignition, combustion and flame characteristics of crude oil droplets. *Energy* 2020; **197**, 117227.

[71] J Wang, Q Zhang, K Liang and J Xu. Micro-explosion enhanced combustion of Jatropha oil/2,5-dimethylfuran (DMF) blended fuel droplets. *Fuel* 2023; **331**, 125807.

[72] G Singh, M Esmaeilpour and A Ratner. The effect of acetylene black on droplet combustion and flame regime of petrodiesel and soy biodiesel. *Fuel* 2019; **246**, 108-116.

[73] HY Setyawan, M Zhu, Z Zhang and D Zhang. Ignition and combustion characteristics of single droplets of a crude glycerol in comparison with pure glycerol, petroleum diesel, biodiesel and ethanol. *Energy* 2016; **113**, 153-159.

[74] YC Liu, Y Xu, MC Hicks and CT Avedisian. Comprehensive study of initial diameter effects and other observations on convection-free droplet combustion in the standard atmosphere for n-heptane, n-octane, and n-decane. *Combustion and Flame* 2016; **171**, 27-41.